

Designing a Sample Stage for Detecting Magnetic Field Feedback of Superconducting Materials Based on Numerical Simulation of Electromagnetic Fields

Ziyan Li and Mengbo Guo

Physics Department, Wuhan University, Wuhan 430072, China

(Dated: June 14, 2022)

To explore the feedback of two-dimensional superconducting materials to the external magnetic field, these materials will be put inside an analyzer chamber under ultra-high vacuum conditions so that the temperature could be easily adjusted to a low temperature below 1K. Therefore, to realize the placement and acceptance of the magnetic field, we designed a device consisting of a drive coil and a receiver coil. The drive coil inputs an external magnetic field to the superconducting material while the receiving coil receives the magnetic field feedback. Superconducting materials are placed right below these coils and the distance between the coil and the material is adjustable. Instead of using commercial COMSOL software to achieve the evaluation of the electromagnetic fields[1], the highlight of the article is to accurately determine the size and parameters of the device based on the first-principles numerical simulation of electromagnetic fields throughout space.

I. EXPERIMENTAL NEEDS

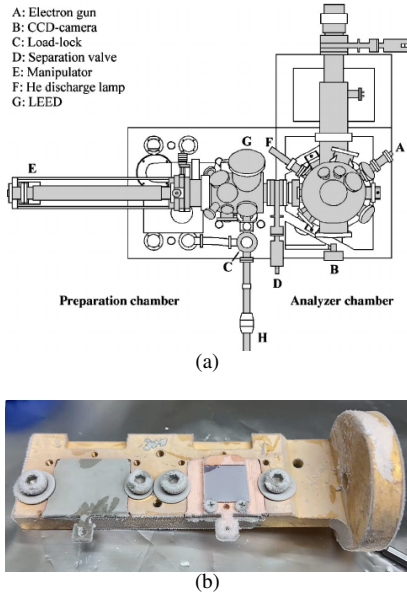


FIG. 1. (a) Top view of the EDA vacuum system and the analyzer chamber with the ellipsoidal display. (b) Sample stage for holding superconducting materials

In experiments to explore the magnetic properties of superconducting materials, ultra-high vacuum and low temperature are often necessary conditions. Therefore, experiments are often carried out in a highly confined space, such as the analyzer chamber[2] in Fig.1(a). The sample material to be tested is placed on the sample stage in Fig.1(b) and sent into the chamber. Once the sample stage is in place, the interior of the chamber must be isolated from the outside world. However, this isolation is not conducive to detecting the feedback of the superconducting material to the applied magnetic field. Because it is not easy for us to apply a magnetic field and it is difficult to collect the magnetic field that the superconducting material feeds back to us.

In order to realize the measurement of the magnetic field in

the closed cavity, we modified the sample stage to facilitate the application of the electromagnetic field and the feedback of the magnetic field from the superconducting material. The key point of designing this new sample stage is how to determine the parameters of this sample stage with high accuracy so that the collected feedback magnetic field is large enough to be measured. In the process of numerical simulation of the magnetic field distribution in space, we refer to the relevant theory of superconducting materials for the feedback of external magnetic field (Meisner effect[3]).

The mirror method[4] is used to estimate feedback in superconducting materials, which is a kind of numerical simulation based on first principles and will be explained later. Compared with the commercial software COMSOL for simulation, its advantage is that it can easily change various parameter settings, and can achieve the same accurate numerical simulation effect as COMSOL.

II. NUMERICAL SIMULATION MODEL

The simulation of the magnetic field in space is based on the Biot-Savart law[5], and combined with the shape and size of the magnetic field source, the magnetic field distribution in the space is calculated to realize the numerical simulation of the magnetic field. In order to simultaneously apply the magnetic field and detect the receiving magnetic field, we place the coil for applying the magnetic field in the middle of the upper and lower coils for receiving the magnetic field, and the sample material to be detected is placed directly under these coils.

A. Drive Coils to Apply the Magnetic Field

The drive coils in the FIG.2 is connected to the external AC power supply. The current in the coil satisfies $I = I_0 \sin(\omega t)$, in which I_0 represents the amplitude of the current and $\omega = 2\pi f$ represents the angular frequency. Using Biot-Savart law, we can find the magnitude of the magnetic field of each coil at a

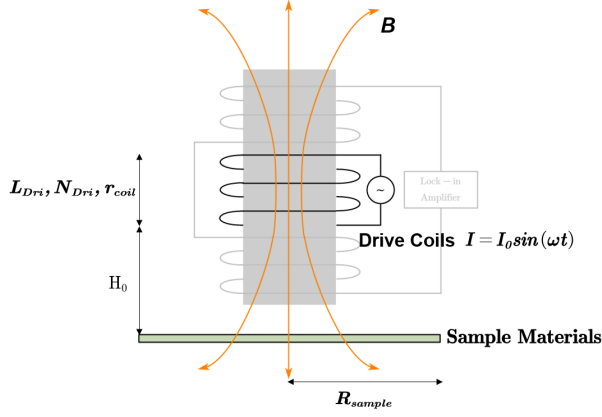


FIG. 2. The drive coil is connected to the power supply and the magnetic field is passed through the sample material directly below

point on its axis at a distance h (the radius of the coil is r_{coil}):

$$B(h) = \frac{\mu_0}{4\pi} \oint \frac{Id\mathbf{r}' \times (\mathbf{r} - \mathbf{r}')}{|\mathbf{r} - \mathbf{r}'|^3} = \frac{\mu_0 I}{4\pi} \sum_{i'=0}^{N_\theta} \frac{r_{coil} d\theta e_{\theta_{i'}} \times (-\mathbf{r}')}{(h^2 + r_{coil}^2)^{\frac{3}{2}}} \quad (1)$$

The equation (1) represents the discretization of Biot-Savart law[6–8], the circumference angle is discretized into N_{theta} parts. The number of the drive coils is N_{Dri} and the overall length of these coils is L_{Dri} . We sum the magnetic field strengths generated by each coil on the axis to obtain the magnetic field distribution on the axis of the drive coils.

$$B_{Drive}(H_0, N_{Dri}) = \sum_{i=0}^{N_{Dri}-1} B(h_0 + i\Delta L) \quad (2)$$

The distance between adjacent coils ΔL in equation(2) is determined by L_{Dri}/N_{Dri} , and L_{Dri} is often deterministic for a model. It is worth noting that h_0 refers to the distance between the bottom of the drive coil and a point on the axis. For example, if we consider the distance from the center of the sample then $h_0 = H_0$ (See FIG. 2)

B. Magnetic Field Feedback and Mirror Method

The magnetic field generated by the driving coil will pass through the sample material directly below. When the temperature drops below the superconducting critical temperature, a surface current will form on the surface of the sample according to the Meissner effect (Appendix A), and the magnetic field generated by the surface current will change the magnetic field in the entire space. Such changes should be accepted and analyzed.

We place two coils with the same parameters in terms of number of turns N_{Rec} , radius r_{coil} , and total length L_{Rec} on the upper and lower sides of the driving coil at equal distances, so as to eliminate the influence of the magnetic field generated by the driving coil on the loop where the receiving coil is located (produced equal large but reverse electromotive force).

The mirror method is used to simulate the magnetic field feedback that occurs when the sample material is superconducting.

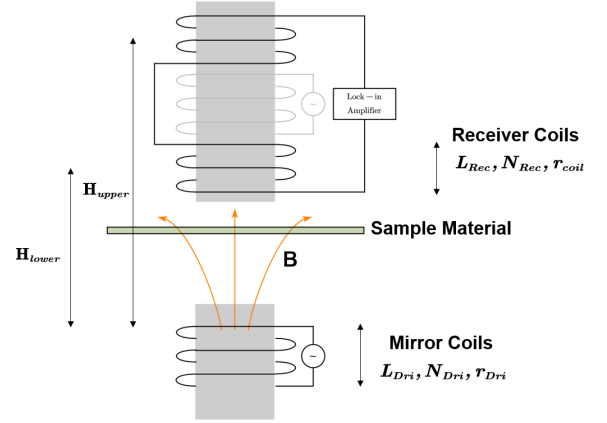


FIG. 3. Above the sample is a receiving coil, which is connected to a current signal amplifier for converting the magnetic field fed back by the superconducting material into current and amplifying it. Below the sample is a mirror image of the drive coil relative to the sample to simulate the feedback magnetic field generated by the sample.

In order to simplify the calculation and ensure that the error is within a controllable range at the same time. We assume that the magnetic field generated by the mirror coil in the receiving coil is constant and can be replaced by the magnetic field generated by the mirror coil in the middle of the receiving coil. The distance between the top of the mirror coil and the middle of the upper and lower coils can be recorded as H_{upper} and H_{lower} respectively.

Using equation (2) and Faraday's law of electromagnetic induction[9, 10], the electromotive force generated by the mirror coil at the upper and lower parts of the receiving coil can be obtained:

$$U_{lower} = -N_{Rec} \frac{d\Phi_{lower}}{dt} = -N_{Rec} \frac{d[B_{Drive}(H_{lower}, N_{Dri})]_z \times \pi r_{coil}^2}{dt} \quad (3a)$$

$$U_{upper} = -N_{Rec} \frac{d\Phi_{upper}}{dt} = -N_{Rec} \frac{d[B_{Drive}(H_{upper}, N_{Dri})]_z \times \pi r_{coil}^2}{dt} \quad (3b)$$

$$\Delta U = |U_{upper} - U_{lower}| \quad (3c)$$

The potential difference shown in equation (3c) can be amplified by the amplifier[11, 12] for subsequent analysis and processing. The existing instrument can measure the potential difference greater than 100nV. That is to say, as long as the measured potential difference is greater than 100nV, it can meet the needs of the experiment.

We substitute all parameters into equation (3c) and we could rewrite it in the way:

$$\Delta U = N_{Rec} f \pi r_{coil}^2 \frac{\mu_0 I_{rms}}{2} \left| \sum_{i=0}^{N_{Dri}-1} \left\{ \sum_{i'=0}^{N_\theta} \frac{r_{coil} d\theta [\vec{e}_{\theta_{i'}} \times (-\vec{r}')]_z}{[(H_{upper} + i \times \frac{L_{Dri}}{N_{Dri}})^2 + r_{coil}^2]^{\frac{3}{2}}} - \sum_{i''=0}^{N_\theta} \frac{r_{coil} d\theta [\vec{e}_{\theta_{i''}} \times (-\vec{r}'')]_z}{[(H_{lower} + i \times \frac{L_{Dri}}{N_{Dri}})^2 + r_{coil}^2]^{\frac{3}{2}}} \right\} \right| \quad (4)$$

TABLE I. Other parameters except N_{Rec} and N_{Dri} , referring to the specifications and sizes of specific experimental equipment. I_{rms} is the rms value of the alternating current in the drive line.

f/kHz	r_{coil}/mm	$I_{rms}/\mu A$	H_{lower}/mm	H_{upper}/mm	L_{Dri}/mm	N_θ
100	2	500	17.5	30.5	8	100

C. Determination of Parameters in the Model

Equation 4 provides many parameters, many of which are inconvenient to change, such as N_{Rec} , N_{Dri} , r_{coil} , ΔL , so this requires us to fix these parameters when designing the model. It is also the meaning of numerical simulation, to determine in advance some parameters that are inconvenient to change in the experiment so as to ensure that the voltage difference received by the receiving coil during the experiment is basically within the range that can be detected. In other words to make ΔU as large as possible. This is the purpose and core of the entire numerical simulation.

In practice, the total length of the coil is always within a certain range, that is to say, L_{Dri} and L_{Rec} should match the size of other experimental equipment. In the process of numerical simulation, only N_{Dri} and N_{Rec} are to be fixed. Therefore, we select appropriate values for other parameters in TABLE I, in order to find the appropriate N_{Dri} and N_{Rec} to maximize the ΔU .

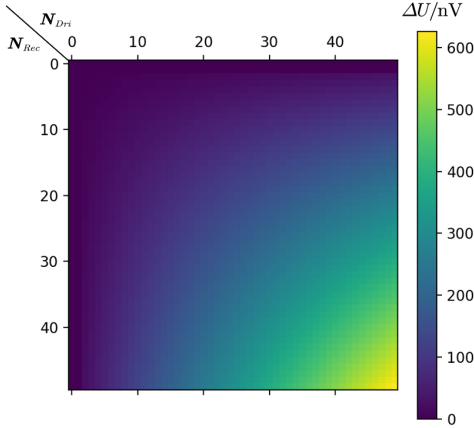


FIG. 4. The result of the numerical calculation of the voltage difference. The voltage difference increases with the increase of N_{Rec} and N_{Dri} . ΔU exceeds 600nV when $N_{Rec} = N_{Dri} = 50$.

FIG 4 shows the results of the numerical calculation of the voltage difference. It can be seen that the calculated voltage difference increases with the number of turns of the driving coils and the receiving coils. However, the number of coil turns should not be too large, otherwise the distance between

the coils will be would be smaller than the size of the coil itself, which is impossible. We can take $N_{Dri}=40$, $N_{Rec}=30$ so the corresponding ΔU is 314.06nV. It is already greater than the detectable 100nV, so this turns ratio is acceptable.

D. The Boundary Effect

However, an important prerequisite for the feasibility of the mirror method is that we can ignore the boundary effect of the sample[13–16], which requires the sample to be large enough. Therefore, we need to estimate the magnitude of the magnetic field generated by the drive coil on the sample surface to ensure the radius R of the sample is larger than a critical value so that the magnetic field generated by the drive coil outside this radius is negligible.

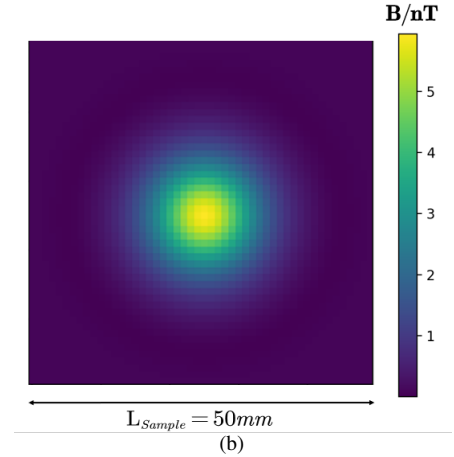
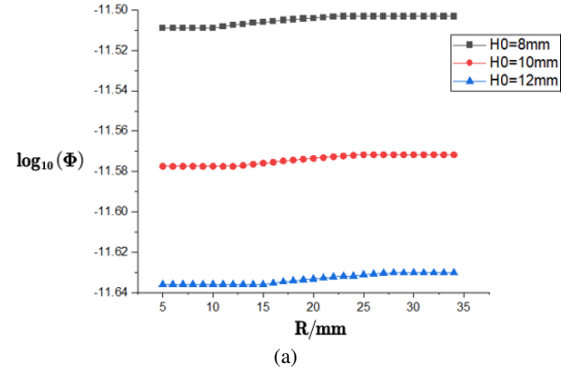


FIG. 5. (a) Convergence of magnetic flux in the sample material given different height $H_0=8mm$, $10mm$ and $12mm$. The abscissa R is the radius of the sample. (b) The magnetic field distribution in the sample plane with length $50mm$ and height $H_0=10mm$

FIG 5(a) proves that the magnetic flux on the sample surface has converged to a fixed value when the sample radius

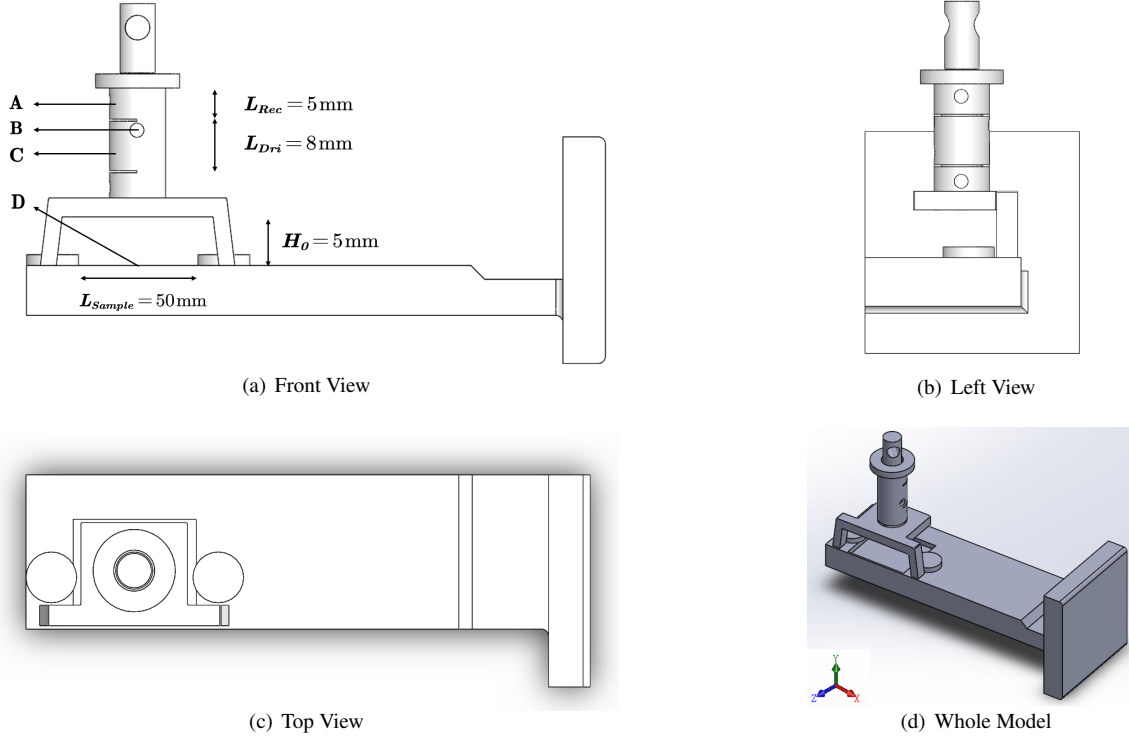


FIG. 6. Three views and 3D model made with SOLIDWORKS software. In order to facilitate the drawing of the three views, the proportions consistent with the stated scale are not taken. (a) The front view, A is the interlayer where the receiving coil is placed; B is the hole for connecting the external power supply; C is the interlayer where the driving coil is placed; D is the sample stage where the sample is placed. (b) The left view. (c) The top view. (d) The view of the whole model.

is greater than 25mm, while FIG 5(b) can prove that when the sample size exceeds this critical value, the magnetic field strength outside this radius is almost negligible.

In fact, there are other numerical simulation methods(details in Appendix B), but they all need to consider the boundary effects of electromagnetic fields.

III. 3D MODELING OF THE DEVICE

Using the parameters given in section IIC, we can use SOLIDWORKS software to draw the 3D model[17, 18] to have an intuitive understanding of the model. The scale of the drawing is not drawn according to the real scale, this is for the convenience of display.

From the main view in FIG 6(a), we can see that the entire model is mainly composed of two parts: a movable cylindrical barrel for loading coils and a sample stage for placing samples. The cylindrical barrel consists of three layers, the middle layer is used to place the driving coil, the upper and lower layers are used to place the receiving coil, and each layer has holes to connect with the external driving circuit or receiving circuit. Just below the cylindrical barrel is the place to carry the sample, and the distance H_0 from the sample to the bottom of the cylindrical barrel can be changed as required.

ACKNOWLEDGMENTS

We wish to acknowledge the support of Professor Jing Shi from Wuhan University, China, encouraging we to finish and perfect this project. We also wish to acknowledge the guidance of Professor Yuanbo Zhang, Master Zhiwei Huang and Master Hengsheng Luo from Fudan University, China, providing the experimental environment and giving some important suggestions.

AUTHOR DECLARATIONS

Conflict of Interest

The authors declare no conflicts of interest.

Author Contributions

Ziyan Li is the major contributor and Mengbo Guo is the minor contributor.

Appendix A: Meissner Effect and London Equation

The Meissner effect refers to the superconductivity that occurs when a material changes from a normal state to a superconducting state with an applied magnetic field. Since this phenomenon[19] was discovered in 1933, people have been looking for relevant theories to explain it, and the London equation[20] proposed by the London brothers is a relatively classic and simple explanation model.

This model assumes that electrons in the superconducting state can be divided into two types: electrons in the normal state and electrons in the superconducting state. The surface current density of the material can be related to the corresponding magnetic vector potential:

$$\mathbf{J} = -\frac{n_s e^2}{m_e} \mathbf{A} \quad (\text{A1})$$

Take the curl for quantities in both sides. Then we can get the relation between current density and magnetic field:

$$\nabla \times \mathbf{J} = -\frac{n_s e^2}{m_e} \mathbf{B} \quad (\text{A2})$$

Combining the Maxwell's equation[21, 22]:

$$\nabla \times \mathbf{B} = \mu_0 \mathbf{J} \quad (\text{A3})$$

Combining all the above formulas to obtain the magnetic field:

$$B(x) = B_0 \exp\left(-\frac{x}{\lambda}\right) \quad (\text{A4})$$

In equation A4, we find that the magnetic field B decreases exponentially, indicating that the magnetic field cannot penetrate the surface of the sample, which is also the reason why the magnetic field B has no vertical component inside the sample.

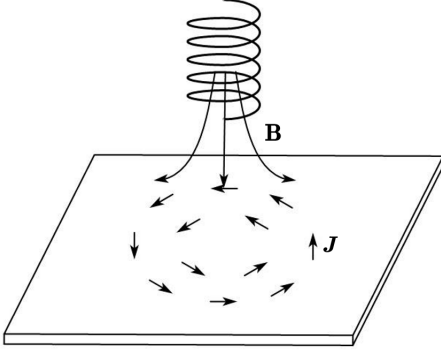


FIG. 7. Surface current generated when a magnetic field is applied directly over a superconducting sample.

As shown in FIG. 7, we can use the formula for surface current to calculate the magnetic field feedback generated by the sample, but this approach is essentially consistent with the mirror method. The mirror method makes the numerical calculation of this model easier, so we do not encourage numerical calculation using the surface current method[23, 24].

Appendix B: Numerical Simulation Based on Annular Current

This is also a method similar to using surface currents to simulate feedback magnetic fields, but unlike Appendix

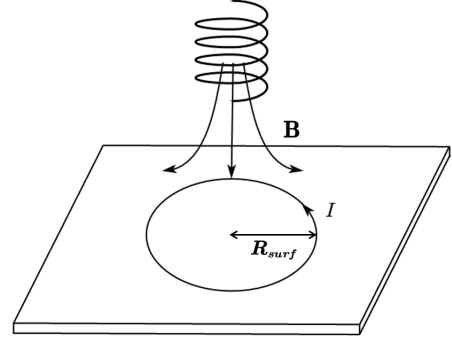


FIG. 8. Ring current used in place of surface current.

A, this method replaces the surface currents with a loop of toroidal currents.

As long as the ring current is determined, the feedback magnetic field of the superconducting material can be calculated by using the Biot-Savart law. The method of confirming the magnitude of the current is to use the sum of the magnetic fluxes generated by the annular current[25, 26] inside it to be equal to the magnetic fluxes generated by the external magnetic field.

Similar to equation 1, taking the center of the ring current as the origin, we can find the vertical component of the magnetic field generated by the ring current at its interior \mathbf{r} :

$$B_{surf}(\mathbf{r}) = \frac{\mu_0 I}{4\pi} \sum_{i'=0}^{N_\theta} \frac{|\mathbf{r}| d\theta \mathbf{e}_{\theta_{i'}} \times (\mathbf{r} - \mathbf{r}')}{|\mathbf{r} - \mathbf{r}'|^3} \quad (\text{B1})$$

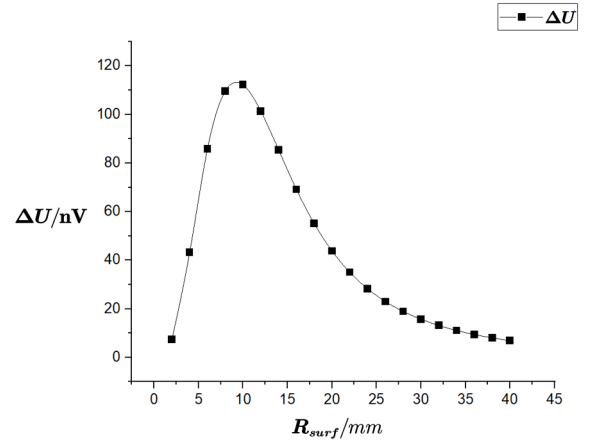


FIG. 9. Ring current used in place of surface current.

Integrating the magnetic field inside the ring current can get the magnetic flux Φ_{surf} generated by the ring current:

$$\Phi_{surf} = \int_0^{R_{surf}} |B_{surf}|_z 2\pi r dr \quad (\text{B2})$$

As for the sum of the magnetic fluxes Φ_{Dri} generated by the driving coil inside the annular current, it is not difficult to obtain it by analogy with equation 2. The derivation process is very simple, so it is not expanded here. Therefore, we can obtain the equation for solving the magnitude of the annular current:

$$\Phi_{surf} + \Phi_{Dri} = 0 \quad (B3)$$

When we take the same parameters as in Table I and choose different radii of the ring current, the potential difference calculated by the method of annular current is shown in FIG. 9.

It can be seen from FIG. 9 that the potential difference calculated by the ring current will vary with the radius R_{surf} taken, indicating that this is not a suitable method. What's more, the maximum value is about 115nV, which is lower than the 314.06nV measured by the mirror method.

-
- [1] S. Liao, W. Li, S. Lin, K. Tang, C. Liou, and C. Tsou, *Sensors and Actuators A: Physical* **269**, 99 (2018).
 - [2] T. Düttemeyer, C. Quitmann, M. Kitz, K. Dörnemann, L. Johansson, and B. Reihl, *Review of Scientific Instruments* **72**, 2638 (2001).
 - [3] H. Essén and M. C. Fiolhais, *American Journal of Physics* **80**, 164 (2012).
 - [4] T. Emig, *Journal of Statistical Mechanics: Theory and Experiment* **2008**, P04007 (2008).
 - [5] T. Charitat and F. Graner, *European Journal of Physics* **24**, 267 (2003).
 - [6] M. Albani and P. Bernardi, *IEEE Transactions on Microwave Theory and Techniques* **22**, 446 (1974).
 - [7] K. Árnason, in *Three-Dimensional Electromagnetics* (Society of Exploration Geophysicists, 1999) pp. 103–118.
 - [8] A. Bossavit, in *Numerical Methods in Electromagnetics*, Handbook of Numerical Analysis, Vol. 13 (Elsevier, 2005) pp. 105–197.
 - [9] G. Giuliani, *EPL (Europhysics Letters)* **81**, 60002 (2008).
 - [10] I. Galili, D. Kaplan, and Y. Lehavi, *American journal of physics* **74**, 337 (2006).
 - [11] A. Uranga, N. Lago, X. Navarro, and N. Barniol, in *2004 IEEE International Symposium on Circuits and Systems (IEEE Cat. No.04CH37512)*, Vol. 4 (2004) pp. IV–21.
 - [12] S. GUIDE, *Power* **18**, 11.
 - [13] D. Pan, S. Lin, L. Li, J. Li, Y. Jin, Z. Sun, and T. Liu, *IEEE Transactions on Industrial Electronics* **67**, 1348 (2020).
 - [14] G. Shou, L. Xia, F. Liu, M. Zhu, Y. Li, and S. Crozier, *IEEE Transactions on Magnetics* **46**, 1052 (2010).
 - [15] T. Evans, R. Moyer, J. Watkins, P. Thomas, T. Osborne, J. Boedo, M. Fenstermacher, K. Finken, R. Groebner, M. Groth, J. Harris, G. Jackson, R. L. Haye, C. Lasnier, M. Schaffer, G. Wang, and L. Zeng, *Journal of Nuclear Materials* **337-339**, 691 (2005), pSI-16.
 - [16] B. W. Yu and S. L. Girshick, *Journal of applied physics* **69**, 656 (1991).
 - [17] P. Schilling and R. Shih, *Parametric Modeling with SOLIDWORKS 2019* (SDC Publications, 2019).
 - [18] J. E. Akin, *Finite element analysis concepts: via SolidWorks* (World Scientific, 2010).
 - [19] P. Anderson and B. Matthias, *Science* **144**, 373 (1964).
 - [20] N. Kaloper and A. Lawrence, *Physical Review D* **95**, 063526 (2017).
 - [21] M. Lax and D. Nelson, *Physical Review B* **13**, 1777 (1976).
 - [22] F. Assous, P. Degond, E. Heintze, P. Raviart, and J. Segre, *Journal of Computational Physics* **109**, 222 (1993).
 - [23] V. Gurevich and R. Laiho, *Physical Review B* **48**, 8307 (1993).
 - [24] V. Gurevich, R. Laiho, and A. Lashkul, *Physical review letters* **69**, 180 (1992).
 - [25] L. Tsai, *IEEE Transactions on Antennas and Propagation* **20**, 569 (1972).
 - [26] D. Webb and G. Hewitt, *International Journal of Multiphase Flow* **2**, 35 (1975).